Supplementary information

Highly Ordered and High-Aspect-Ratio Au Nanopatterns Directly Fabricated on Cu for Efficient Anode-Less Li Metal Batteries

Hyunju Jung[1,2], Hee-Tae Jung[1,2]*

[1] Department of Chemical and Biomolecular Engineering, Korea Advanced Institute of Science and Technology (KAIST), Daejeon, 34141, Republic of Korea.

[2] KAIST-UC Berkeley-VNU Global Climate Research Center, Korea Advanced Institute of Science and Technology (KAIST), Daejeon, 34141, Republic of Korea
E-mail: heetae@kaist.ac.kr

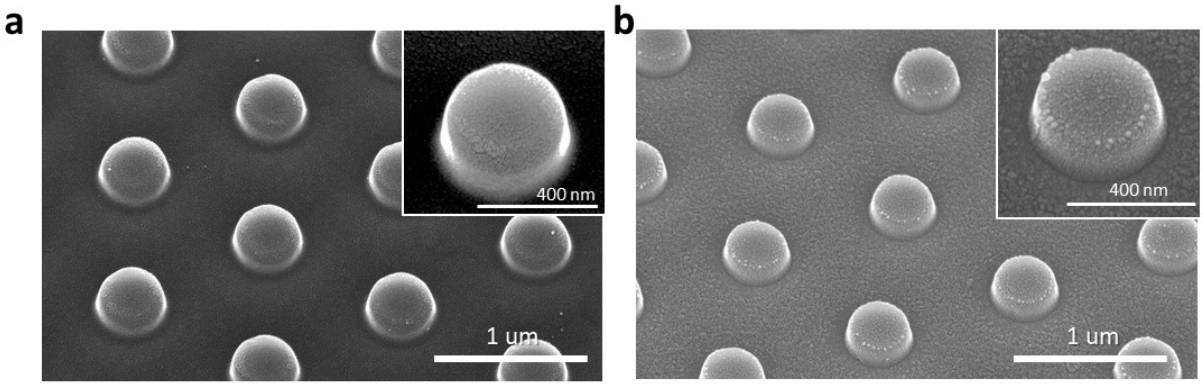

Figure S1. Scanning Electron Microscope (SEM) images of polystyrene (PS) prepatterns directly formed on Cu foil. (a) PS prepatterns after nanoimprint lithography, showing the uniform pattern formation on the substrate; (b) PS patterns after the removal of residual PS using reactive ion etching (RIE), illustrating a clean and well-defined pattern on the Cu foil.

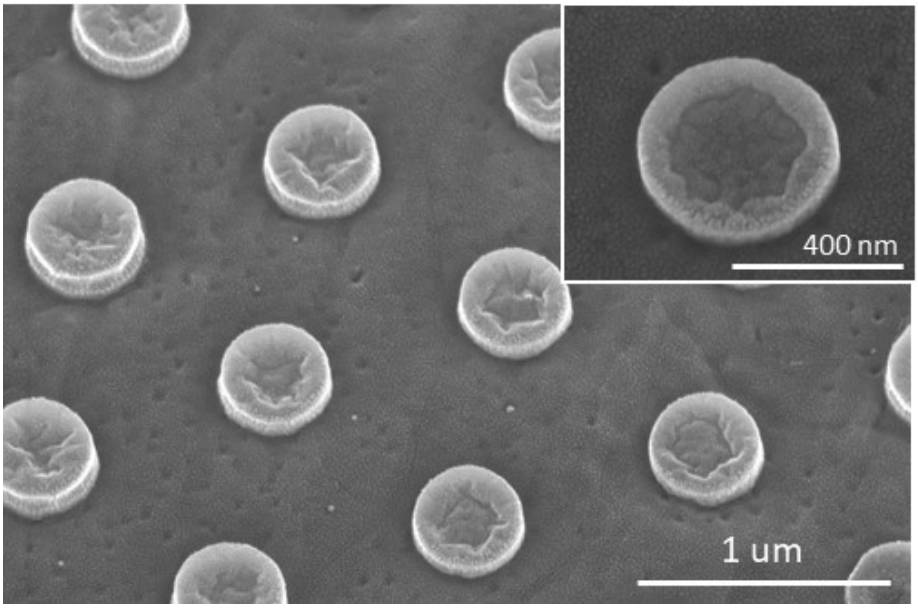

Figure S2. SEM images of disk-shaped Au patterns formed after Ar^+ ion bombardment. The exposed Au regions were etched away, leaving the Au beneath the PS prepatterns intact, resulting in well-defined disk-shaped structures

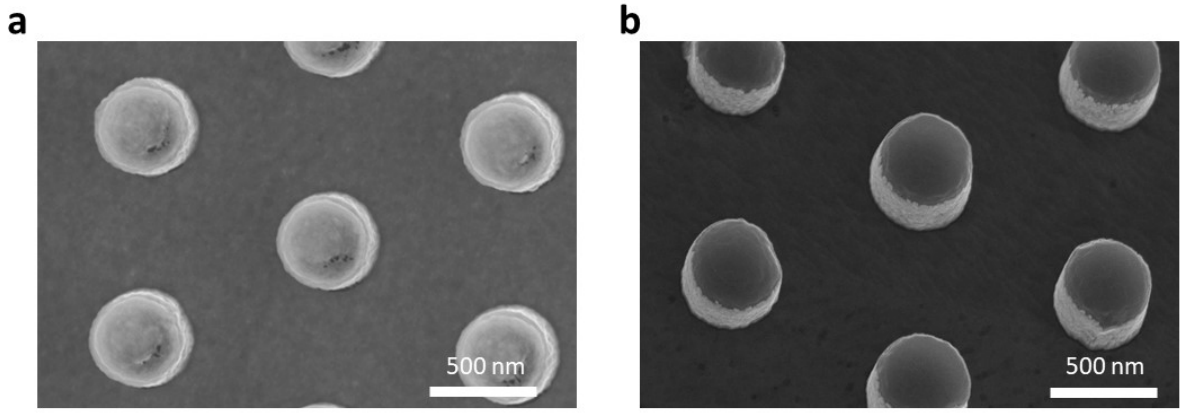

Figure S3. SEM images illustrating the fabrication process of hole-cylinder Au patterns. (a) Au deposition onto PS prepatterns. (b) Formation of hole-cylinder Au patterns following Ar^+ ion bombardment, with the Au conformally attached to the prepattern.

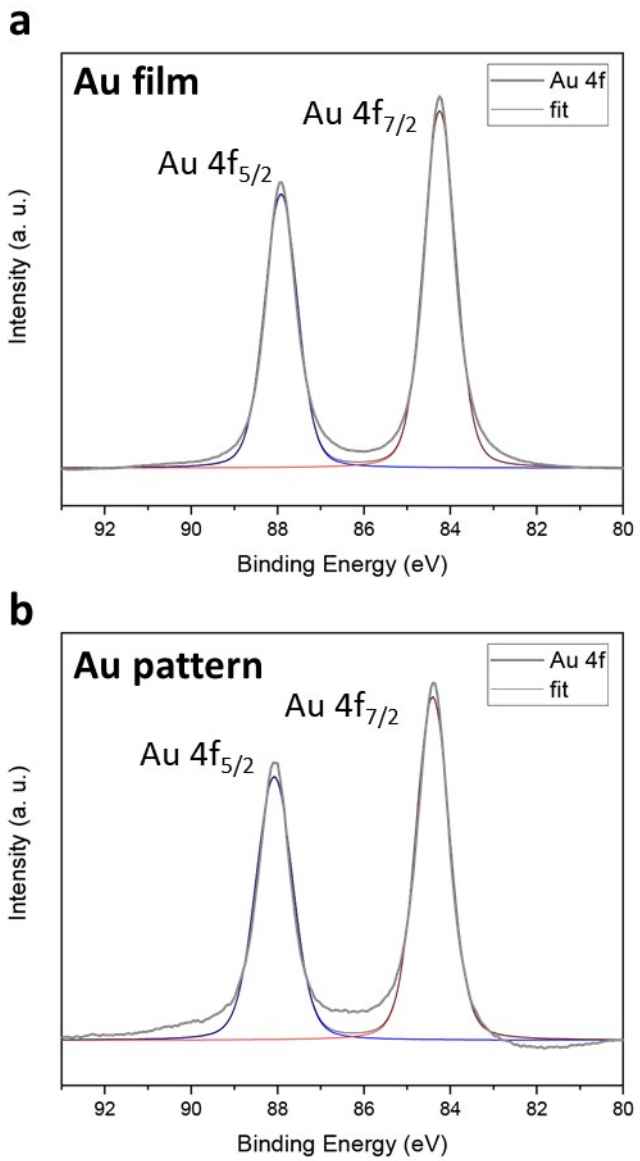

Figure S4. X-ray photoelectron spectroscopy (XPS) spectra confirming the metallic state of Au 4f. (a) Au film deposited on Cu current collector and (b) the 3D Au hole-cylinder nanopattern on Cu current collector. In both cases the Au $4f_{7/2}$ and Au $4f_{5/2}$ peaks appear at ~84.0 eV and ~87.7 eV, respectively, with no detectable higher-binding-energy shoulders, indicating that Au remains predominantly in the metallic (Au^0) state with negligible oxidation.

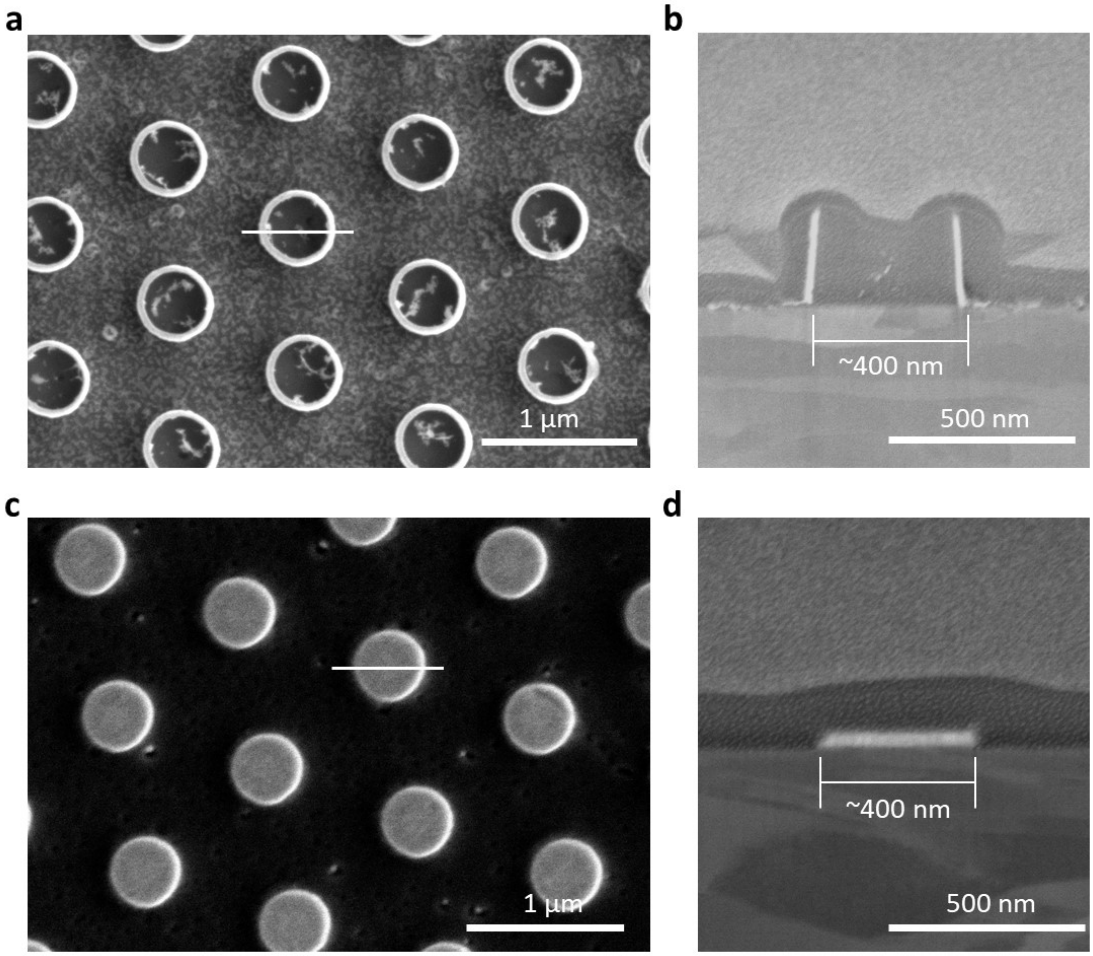

Figure S5. Cross-sectional analysis of Au nanopatterns on Cu foil. (a) Top view and (b) side view of the hole-cylinder Au patterned Cu current collector. (c) top view and (d) side view of the flat disk shaped Au patterned Cu current collector. The white line in (a, c) indicates the position of the cross-section.

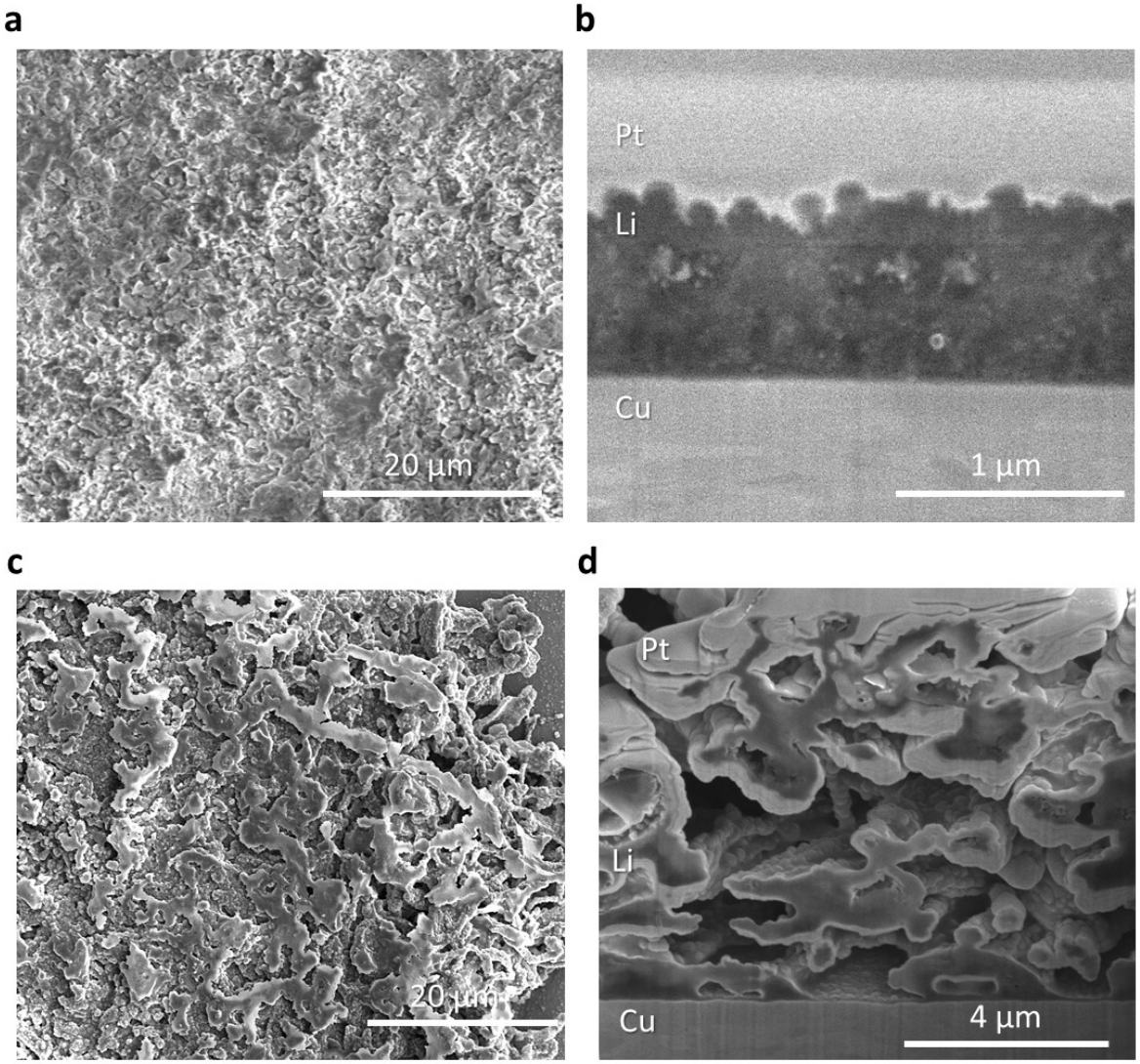

Figure S6. Cross-sectional analysis of lithium deposition on current collectors. (a) Top view and (b) side view of the hole-cylinder Au patterned anode after lithiation. (c) top view and (d) side view of the bare Cu electrode after lithiation.

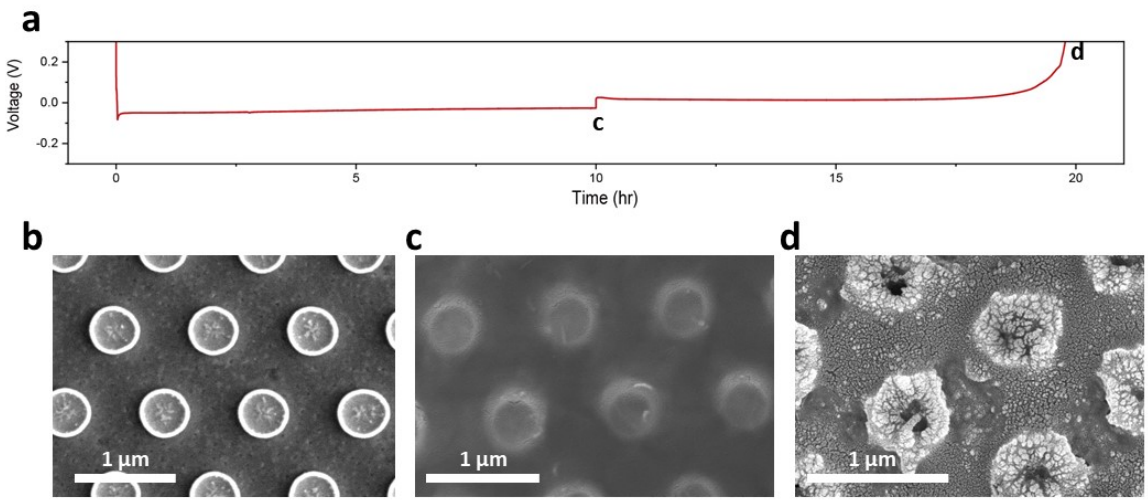

Figure S7. (a) Voltage profile for Li plating (5 mAh cm^{-2}) and subsequent stripping (5 mAh cm^{-2}) at 0.5 mA cm^{-2} in 1 M LiTFSI/DOL–DME (1:1, v/v) with 1 wt % $LiNO_3$. (b–d) Ex-situ FE-SEM images illustrating morphology evolution on the Au hole-cylinder nanopatterned Cu current collector: (b) pristine surface before Li deposition, (c) after full Li plating (5 mAh cm^{-2}), and (d) after stripping to 1.0 V.

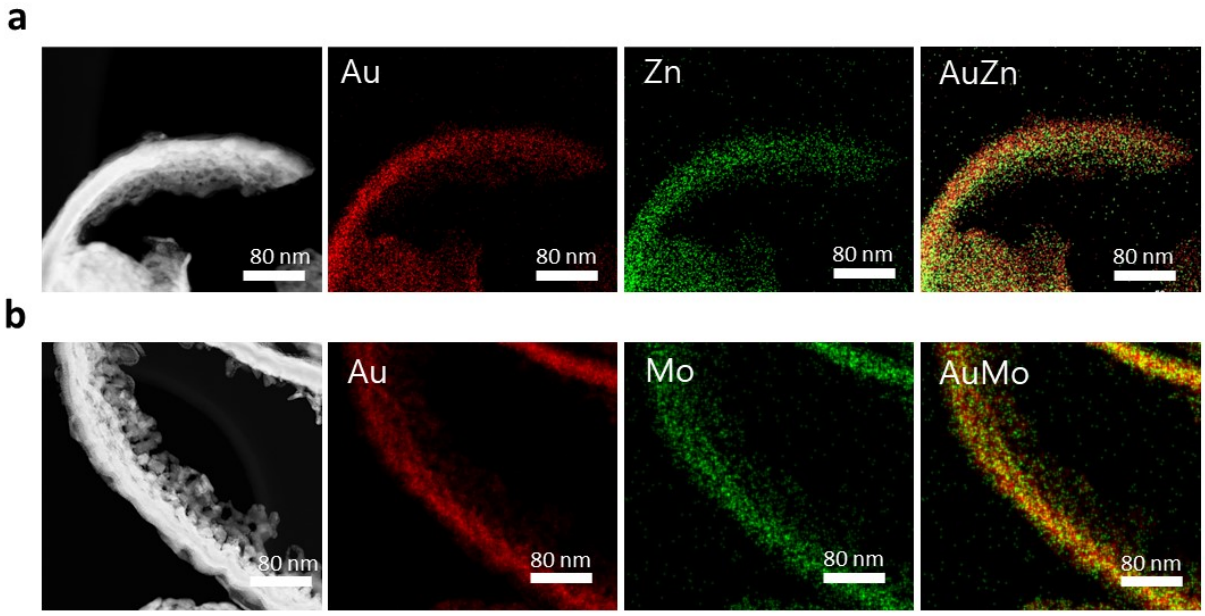

Figure S8. EDS mapping of the multi-metal compositions in the fabricated patterns. (a) uniform distribution of Au and Zn within the hole-cylinder pattern. (b) Distribution of Au and Mo within the pattern. The results confirm the effective mixing of metals achieved through secondary sputtering during the Ar^+ ion bombardment step.